Supporting Information

Contents

Experimental Section

Additional experimental procedures

Synthesis of bis(4-methylpiperidino)acetylene (2). The literature protocol[1] was adapted as follows. A solution of ^{n}BuLi (2.5 M in hexane, 6.53 mL, 16.35 mmol, 1.1 equiv) was added dropwise to a stirred solution of 1,1-di(4-methylpiperidino)-2,2-dibromoethene (5.65 g, 14.86 mmol, 1 equiv) in hexane (60 mL), which resulted in the formation of a white precipitate (LiBr). After 30 min the excess ^{n}BuLi was quenched with dimethylformamide (1 mL), and the mixture was filtered over a pad of Celite® and washed with hexane (10 mL + 2 × 5 mL). The yellow filtrate was collected in a silylated flask and the volatiles were removed in high vacuum, affording a yellowish residue. After bulb-to-bulb distillation under low pressure (3 Pa) **2** was obtained as a colourless crystalline solid and stored in a silylated flask at −30 °C. Yield: 79% (2.57 g). The spectroscopic data are in agreement with the literature.[1]

One-pot synthesis of bis(diethylamino)acetylene (3). The literature protocols[2,3] were adapted as follows. To a precooled (−80 °C) solution of trichloroethylene (6.570 g, 50.0 mmol) in Et$_2$O (50 mL) a solution of lithium diethylamide (3.954 g, 50.0 mmol, 1.0 equiv) in Et$_2$O (50 mL) was carefully added dropwise over a period of 45 min. After addition was completed, the orange solution was stirred for 2 h and allowed to warm gradually to room temperature, leaving a turbid brown mixture. The mixture was cooled again to −80 °C and, under exclusion of light, a solution of lithium diethylamide (3.954 g, 50.0 mmol, 1.0 equiv) in Et$_2$O (50 mL) was slowly added over a period of 45 min. The mixture was stirred for 1 h and allowed to warm gradually to 0 °C, resulting in a brown mixture. At this temperature, the solvent was partially removed (approx. 100 mL) at low pressure (besides the solvent, a yellow substance was collected in the cold trap that decomposes in contact with air). The deep maroon mixture was cooled to −80 °C again and, under exclusion of light, a solution of lithium diethylamide (4.349 g, 55.0 mmol, 1.1 equiv) in Et$_2$O (50 mL) was slowly added over 45 min. The reaction mixture was then allowed to warm gradually to 0 °C and the solvent was partially removed (approx. 100 mL). The brown mixture was filtered through a Celite®-pad and washed with Et$_2$O (4 × 5 mL). The solvent was removed at 0 °C and the brown residue was purified by bulb-to-bulb distillation (40–70 °C, 5 Pa) affording **3** as a pale yellow liquid. Yield: 48% (4.00 g). The spectroscopic data are in agreement with the literature.[3]

Attempted metathesis of diphenylacetylene and the diaminoacetylene 2. To a stirred solution of diphenylacetylene (18 mg, 100 µmol) and **2** (22 mg, 100 µmol) in C$_6$D$_6$ (0.6 mL) was added 1 mol% of **1** (0.8 mg, 1 µmol), resulting in an immediate colour change to red. The reaction mixture was analysed by NMR spectroscopy, revealing only the presence of the starting materials even after 24 h, heating at 50 °C or further addition of 1 mol% of **1**.

X-ray crystal structure determinations

Table S1. Crystallographic data for compound **4**.

empirical formula	$C_{36}H_{44}F_{18}MoN_2O_3$	V (Å³)	2034.68(19)
M_w	990.67	Z	2
wavelength (Å)	1.54184	ρ_{calc} (Mg m⁻³)	1.617
T (K)	100(2)	μ (mm⁻¹)	3.744
cryst size (mm³)	0.20 × 0.08 × 0.05	$F(000)$	948
cryst system	triclinic	reflections collected	92647
space group	$P\bar{1}$	indep. reflections (R_{int})	8408 (0.0810)
a (Å)	11.2300(6)	Parameters	569
b (Å)	12.6831(6)	Restraints	112
c (Å)	15.8296(10)	Goodness-of-fit on F^2	1.038
α (°)	101.495(5)	R_1 ($I > 2\sigma(I)$)	0.0492
β (°)	110.382(6)	wR_2 (all reflections)	0.1279
γ (°)	95.857(4)	max and min $\Delta\rho$ (e Å⁻³)	0.777 and −1.421

Table S2. Crystallographic data for compound **5**.

empirical formula	$C_{32}H_{40}F_{18}MoN_2O_3$	V (Å³)	1921.25(11)
M_w	938.60	Z	2
wavelength (Å)	1.54184	ρ_{calc} (Mg m⁻³)	1.622
T (K)	100(2)	μ (mm⁻¹)	3.927
cryst size (mm³)	0.18 × 0.15 × 0.04	$F(000)$	948
cryst system	triclinic	reflections collected	119615
space group	$P\bar{1}$	indep. reflections (R_{int})	8009 (0.0556)
a (Å)	12.5635(5)	Parameters	555
b (Å)	12.6072(4)	Restraints	98
c (Å)	12.7731(4)	Goodness-of-fit on F^2	1.040
α (°)	88.000(2)	R_1 ($I > 2\sigma(I)$)	0.0318
β (°)	73.097(3)	wR_2 (all reflections)	0.0833
γ (°)	82.987(3)	max and min $\Delta\rho$ (e Å⁻³)	0.793 and −0.876
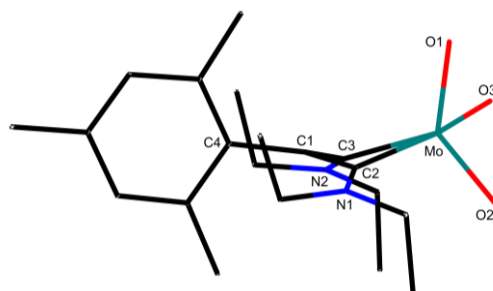
Figure S1. Side view of the structure of complex **5**. The $(CF_3)_2MeC$-groups and hydrogen atoms are omitted for clarity.

Table S3. Comparison of selected bond lengths (in Å) between complexes **4**, **5**, and **6**.

Bond	4	5	6
Mo–C2	2.166(3)	2.1422(2)	2.202(4)
Mo–C3	2.138(3)	2.1203(19)	2.228(4)
Mo–O1	2.089(2)	1.9413(14)	–
Mo–O2	1.936(2)	1.9084(15)	–
Mo–O3	1.912(3)	2.0787(15)	–
C1–C2	1.423(5)	1.433(3)	1.457(5)
C1–C3	1.413(4)	1.413(3)	1.367(5)
C1–C4	1.499(4)	1.499(3)	1.485(6)
N1–C2	1.323(4)	1.324(3)	1.316(5)
N2–C3	1.322(4)	1.324(3)	
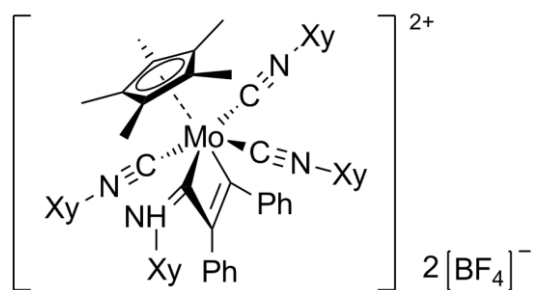
Figure S2. Structure of complex **6**.[4] Xy = 2,6-dimethylphenyl.

NMR studies

Variable temperature NMR spectroscopy of 4
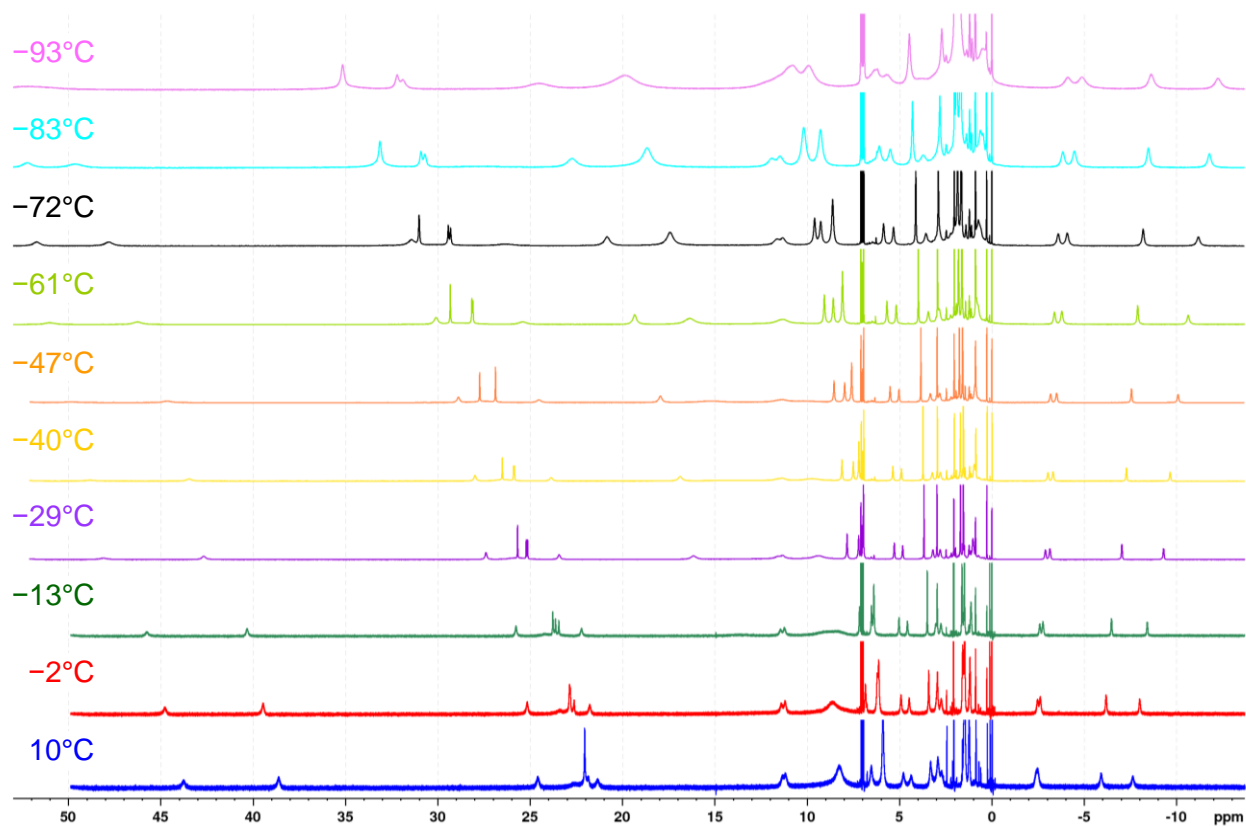
Figure S3. VT ^{1}H NMR of **4** in toluene-d_8.

Table S4. ^{1}H NMR shifts (in ppm) of **4a** (major isomer) in toluene-d_8 at various temperatures.

T (°C)	mesityl m-C*H*[a]	o-C*H*$_3$[a]	p-C*H*$_3$	4-C*H*$_3$	4-C*H*	4-methyl-piperidino 3,5-C*H*$_2$[c]	2,6-C*H*$_2$[c]	(CF$_3$)$_2$(C*H*$_3$)CO[g]
−93	31.9, 32.2	10.8[b]	4.5	1.8	0.5	−8.6, −4.9, −,[d] 6.3	11.6,[e] 35.3, 51.7	12.3, 24.5
−83	30.7, 30,9	10.2[b]	4.3	1.7	0.6	−8.5, −4.5, −,[d] 6.1	11.5,[e] 33.3, 49.6	11.9, 22.7
−72	29.3, 29,4	9.3, 9.6	4.1	1.7	0.7	−8.2, −4.1, 2.9, 5.9	11.3,[e] 31.4, 47.8	11.6, 20.8
−61	28.1, 28.2	8.6, 9.1	4.0	1.6	0.8	−7.9, −3.8, 2.8, 5.7	11.4,[e] 30.1, 46.3	11.1, 19.3
−47	26.9[b]	8.0, 8.6	3.9	1.6	0.9	−7.6, −3.5, 2.8, 5.5	11.4,[e] 28.9, 44.7	10.4, 18.0
−40	25.9, 25.9	7.5, 8.1	3.8	1.6	1.0	−7.3, −3.3, 2.8, 5.4	11.5,[e,f] 28.0, 43.5	9.7, 16.9
−29	25.1, 25.2	7.2, 7.8	3.7	1.5	1.0	−7.0, −3.2, 2.8, 5.3	11.4,[e,f] 27.4, 42.7	9.4, 16.1
−13	23.5, 23.6	6.5, 7.2	3.5	1.5	1.1	−6.5, −2.8, 2.8, 5.0	11.3,[e,f] 25.8, 40.3	8.7, 13.6
−2	22.6, 22.8	6.2, 6.9	3.4	1.5	1.2	−6.2, −2.6, 2.7, 4.9	11.3,[e,f] 25.2, 39.5	8.6, 12.7
10	21.9, 22.1	6.0, 6.6	3.3	1.5	1.3	−5.9, −2.5, 2.7, 4.8	11.3,[e,f] 24.6, 38.6	8.3, −[h]

[a] Two inequivalent positions. [b] Overlapped resonances. [c] All four hydrogen atoms in these positions are diastereotopic, each resonance integrates to 2H. [d] One resonance is missing because of overlap. [e] Presumed assignment; probably two resonances (4H). [f] Apparent doublet. [g] Presumed assignments, since the integrals do not fit for all temperatures. The first resonance probably integrates to 6H, and the second probably integrates to 3H. [h] One resonance is not observable because of line broadening.

Table S5. ^{1}H NMR shifts (in ppm) of **4b** (minor isomer) in toluene-d_8 at various temperatures.

T (°C)	mesityl m-C*H*	o-C*H*$_3$	p-C*H*$_3$	4-C*H*$_3$	4-C*H*	4-methyl-piperidino 3,5-C*H*$_2$[b]	2,6-C*H*$_2$[c]	(CF$_3$)$_2$(C*H*$_3$)-CO[e]
−93	35.2	9.9	2.7	2.0	0.4	−12.3, −4.1, 3.8, 5.7	28.7, −,[d] 52.7[a]	19.8
−83	33.1	9.3	2.8	1.9	0.5	−11.8, −3.9, 3.7, 5.5	27.6, −,[d] 52.2	18.7
−72	31.0	8.6	2.9	1.9	0.6	−11.2, −3.6, 3.6, 5.3	26.3, −,[d] 51.7	17.4
−61	29.3	8.1	2.9	1.8	0.7	−10.6, −3.4, 3.4, 5.2	25.4, *29*, 51.0	16.4
−47	27.8	7.6	3.0	1.8	0.9	−10.1, −3.2, 3.3, 5.0	24.5, *28*, 49.9	15.2
−40	26.5	7.2	3.0	1.7	1.0	−9.6, −3.0, 3.2, 4.9	23.9, *26*, 48.8	14.0
−29	25.6	7.0	3.0	1.7	1.0	−9.3, −2.9, 3.2, 4.8	23.4, *26*, 48.1	−[f]
−13	23.8	6.4	3.0	1.6	1.1	−8.4, −2.6, 3.0, 4.6	22.2, *24*, 45.8	−[f]
−2	22.9	6.1	3.0	1.6	1.2	−8.0, −2.5, 3.0, 4.5	21.8, *23*, 44.8	−[f]
10	22.0[a]	5.9	2.9	1.5	1.3	−7.6, −2.4, 2.9, 4.4	21.4, *22*, 43.8	−[f]

[a] Estimated value because of overlap. [b] All four hydrogen atoms in these positions are diastereotopic, each resonance integrates to 2H. [c] Presumed assignments because of overlap. Four resonances are expected because of the diastereotopic hydrogen atoms in these positions: Two resonances (2 × 2H) can be easily identified, whereas the other two are very broad and overlap with themselves and other resonances; an estimate of the chemical shift is given here in italics. [d] One resonance is missing because of overlap. [e] Presumed assignments, since the integral do not fit for all temperatures. [f] Resonance not observable because of line broadening.

*NMR spectra of **4** at −29 °C*
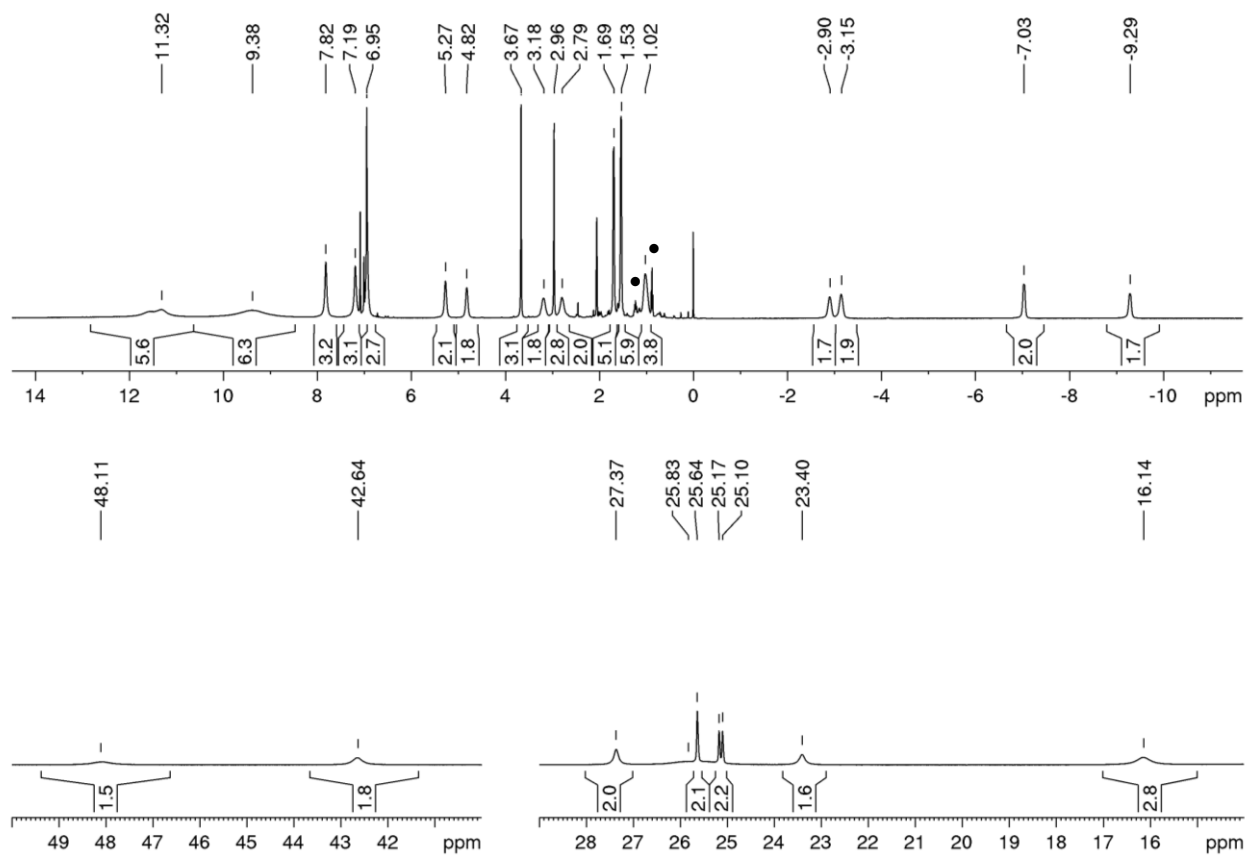
Figure S4. ^{1}H NMR spectrum (divided in three segments) of **4** at −29 °C in toluene-d_8.
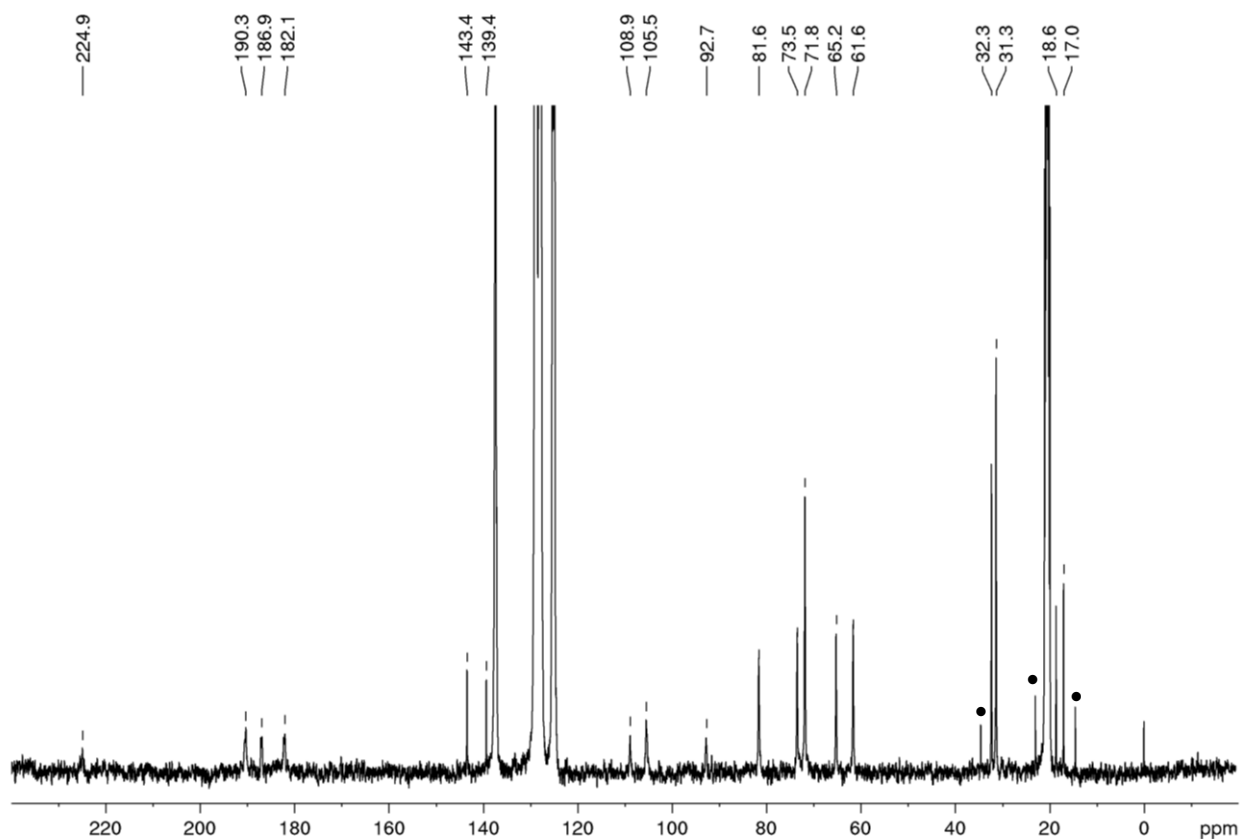
• = pentane.

Figure S5. $^{13}C\{^1H\}$ NMR spectrum of **4** at −29 °C in toluene-d_8. • = pentane.
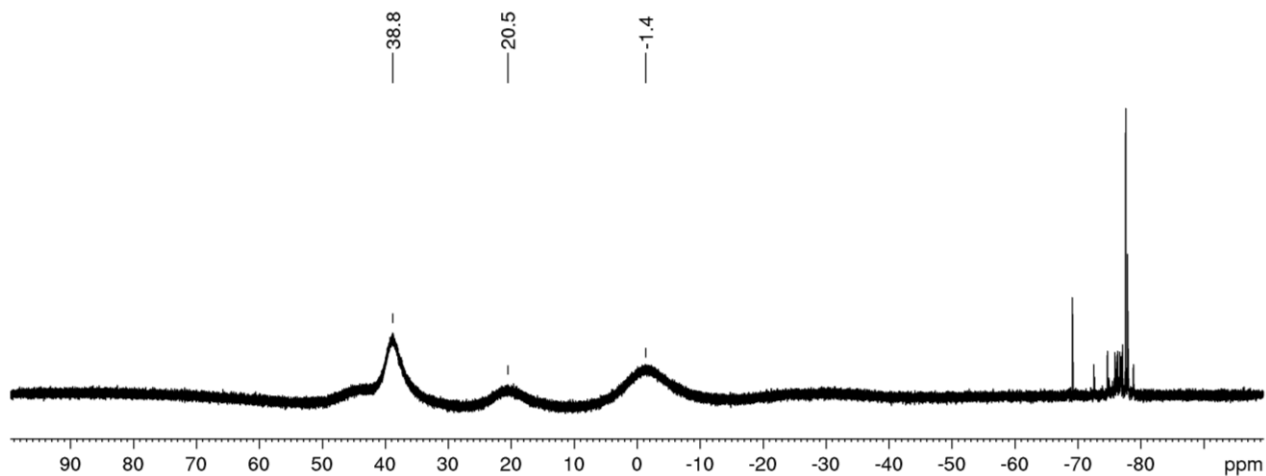
Figure S6. $^{19}F\{^1H\}$ NMR spectrum of **4** at −29 °C in toluene-d_8. The signals around −70 ppm and −80 ppm correspond to small amounts of decomposition products.

Stereoisomers of 4

Figure S7. Stereoisomers of compound **4**.

Variable temperature NMR spectroscopy of 5
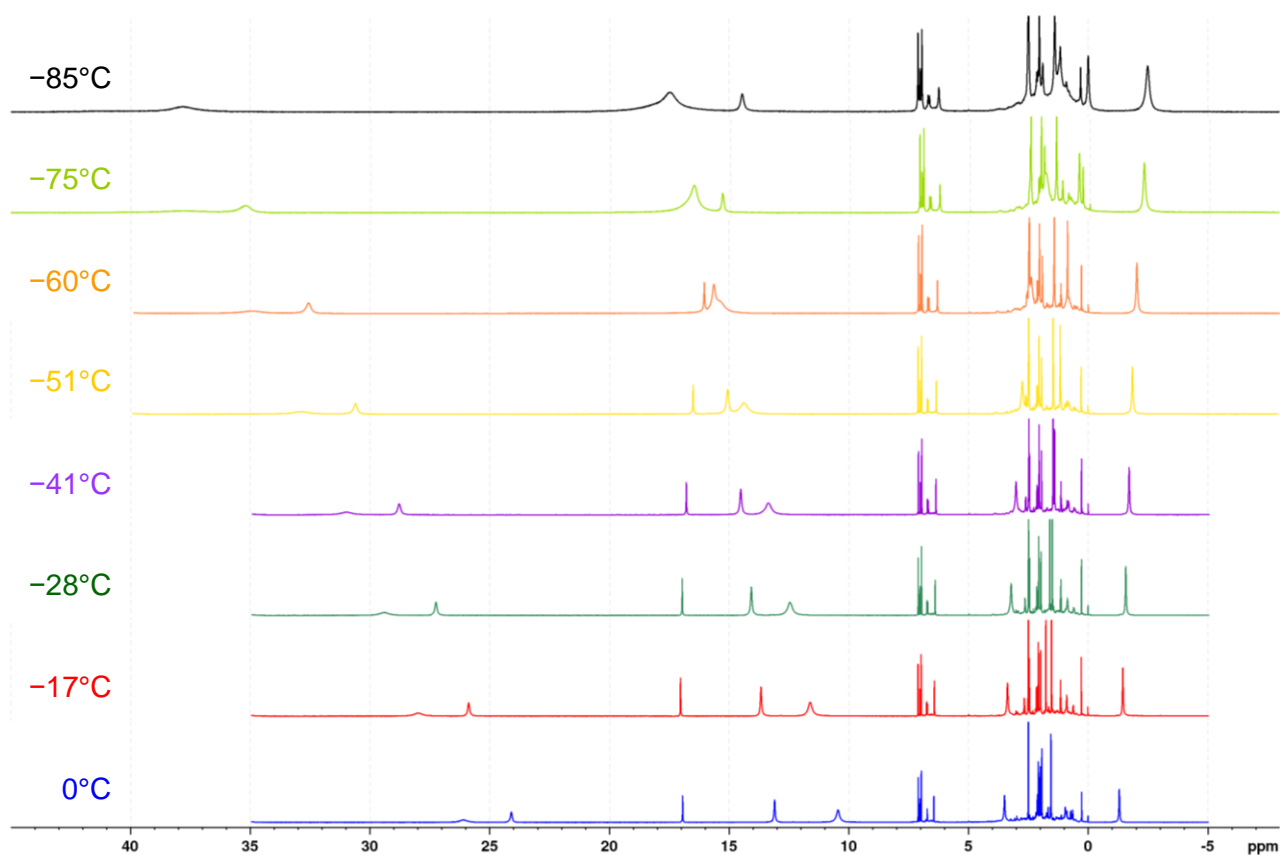
Figure S8. VT ^{1}H NMR of **5** in toluene-d_8.

Table S6. ^{1}H NMR shifts (in ppm) of **5** in toluene-d_8 at various temperatures.

	mesityl			diethylamino		$(CF_3)_2(CH_3)CO$
T (°C)	m-CH	o-CH_3	p-CH_3	CH_3	CH_2	
−85	14.4	1.2	0.0	17.5, −2.5	40.4, 37.8	18.0
−75	15.3	1.8	0.5	16.5, −2.3	37.7, 35.2	16.9
−60	16.0	2.4	0.9	15.6, −2.0	34.9, 32.6	15.4
−51	16.5	2.7	1.2	15.0, −1.9	32.9, 30.6	14.4
−41	16.8	3.0	1.4	14.5, −1.7	31.0, 28.8	13.4
−28	17.0	3.2	1.6	14.1, −1.6	29.4, 27.3	12.5
−17	17.0	3.4	1.8	13.7, −1.5	28.0, 25.9	11.6
0	16.9	3.5	1.9	13.1, −1.3	26.1, 24.1	10.4
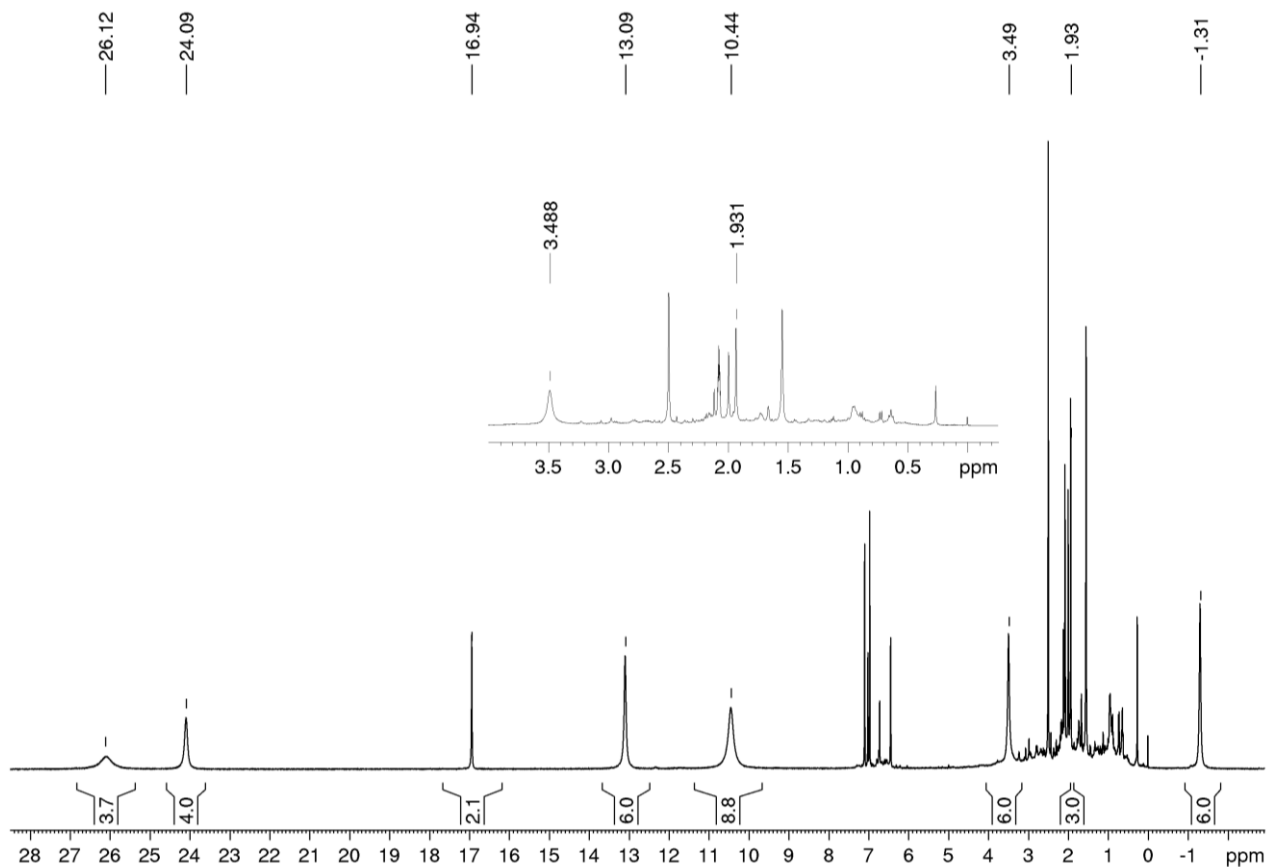
Figure S9. ^{1}H NMR spectrum of **5** at 0 °C in toluene-d_8. Only the paramagnetic resonances are highlighted. The segment between 0 ppm and 4 ppm is amplified for clarity.
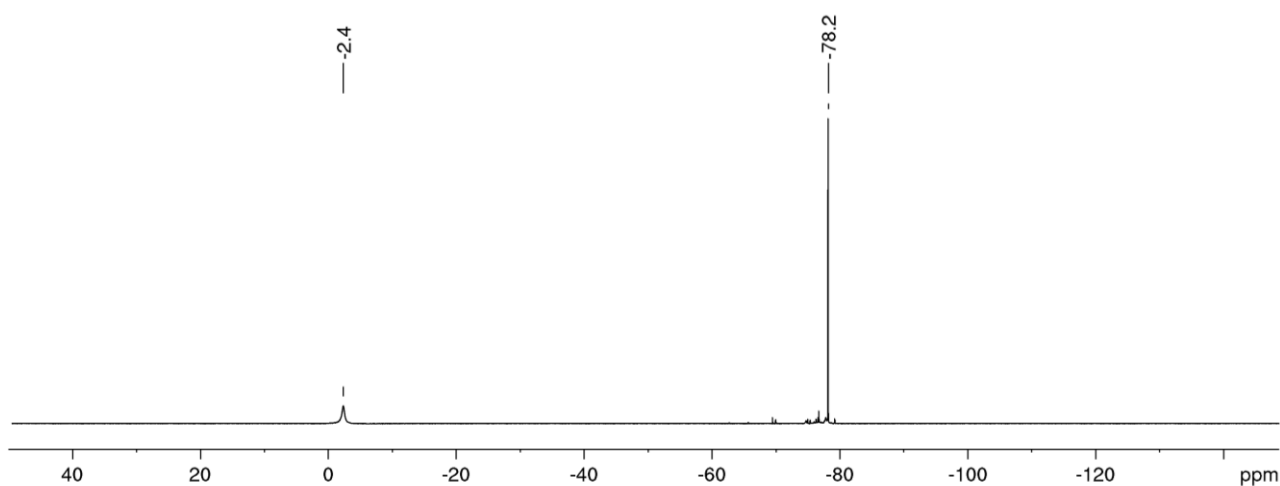
Figure S10. ^{19}F{^{1}H} NMR spectrum of **5** at 0 °C in toluene-d_8. The signal at −78.2 ppm corresponds either to complex **1** or to the side product **I6**.

Solid-state magnetic susceptibility studies
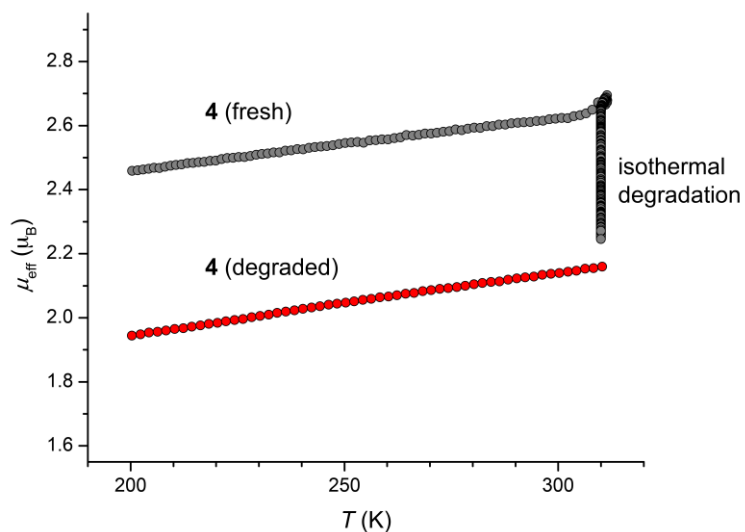
Figure S11. Effective magnetic moment (μ_{eff}) vs. T plots for complex **4** before (dark grey) and after (red) isothermal degradation at $T = 310$ K, measured with an externally applied magnetic field of $B_{ext} = 0.1$ T.
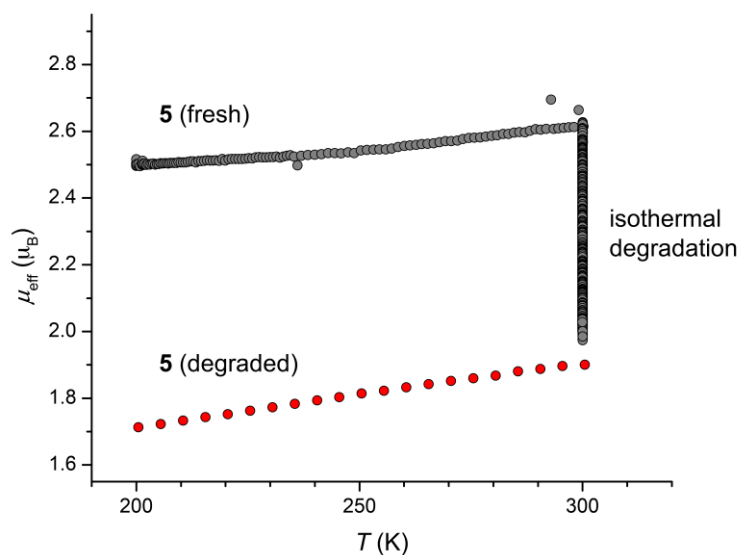
Figure S12. Effective magnetic moment (μ_{eff}) vs. T plots for complex **5** before (dark grey) and after (red) isothermal degradation at $T = 300$ K, measured with an externally applied magnetic field of $B_{ext} = 0.1$ T.
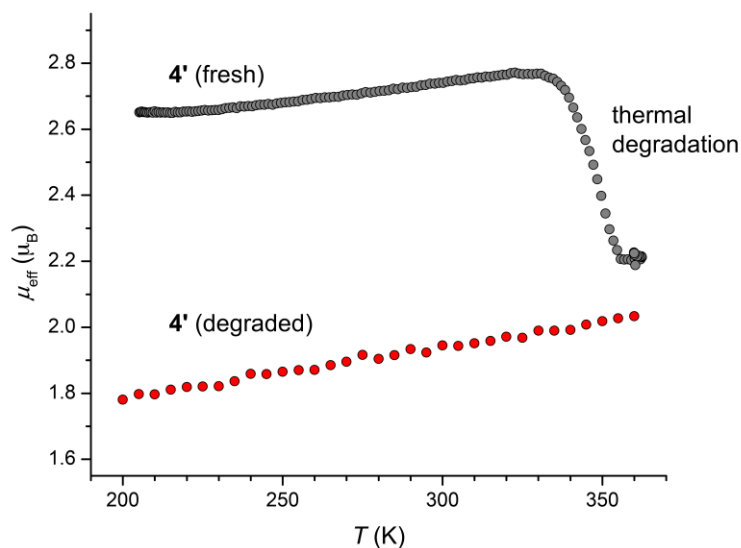
Figure S13. Effective magnetic moment (μ_{eff}) vs. T plots for complex **4'** before (dark grey) and after (red) thermal degradation above $T = 300$ K, measured with an externally applied magnetic field of $B_{ext} = 0.1$ T.
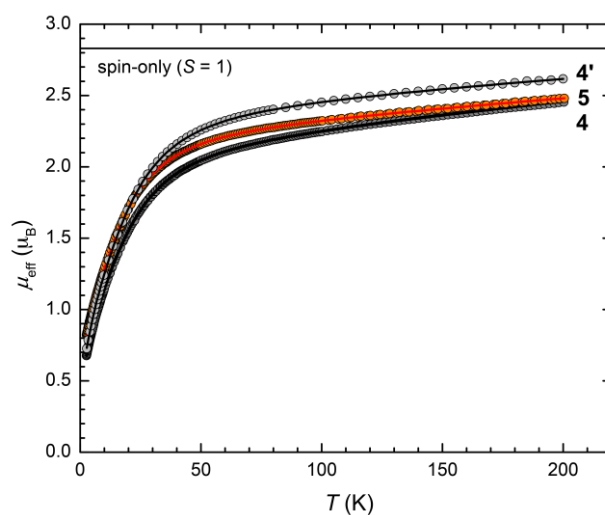
Figure S14. Effective magnetic moment (μ_{eff}) vs. T plots for complexes **4** (dark grey), **4'** (grey) and **5** (orange) measured with an externally applied magnetic field of $B_{ext} = 0.1$ T; symbols: experimental data; lines: fit on the basis of a modified spin Hamiltonian approach (see article main text).
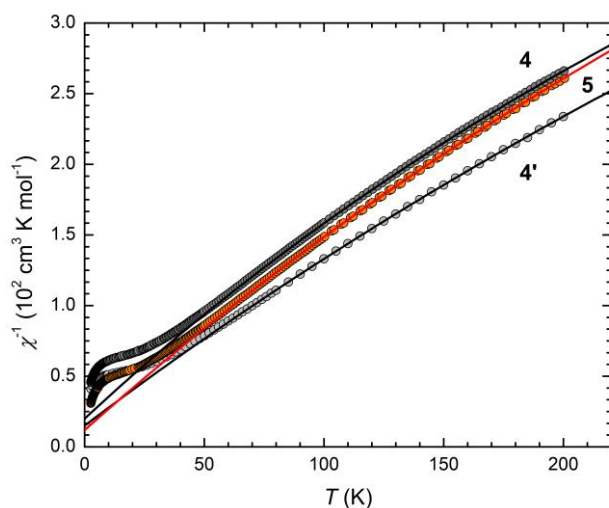
Figure S15. Inverse magnetic susceptibility (χ^{-1}) vs. T plots for complexes **4** (dark grey), **4'** (grey) and **5** (orange) measured with an externally applied magnetic field of B_{ext} = 0.1 T; symbols: experimental data; lines: fit on the basis of the model described in eq. 1.

Table S7. Parameters determined on the basis of different Curie-Weiss models (cf. eq. 1) with (I) D_{TIP} = 0; (II) D_{TIP} values taken from Table S8; (III) with D_{TIP} as a free fit parameter.

model	compound	C (cm³ K mol⁻¹)	θ (K)	D_{TIP} (10⁻⁴ cm³ mol⁻¹)	μ_{eff} (μ_B)
I	**4**	0.893(4)	−41.0(7)	0[a]	2.67
	4'	0.972(5)	−29.1(9)	0[a]	2.79
	5	0.866(3)	−28.3(6)	0[a]	2.63
II	**4**	0.607(1)	−9.9(1)	9.63[a]	2.20
	4'	0.764(1)	−10.2(1)	7.16[a]	2.47
	5	0.667(1)	−8.5(1)	6.92[a]	2.30
III	**4**	0.633(2)	−12.4(2)	8.8(6)	2.25
	4'	0.780(7)	−11.6(6)	6.6(2)	2.50
	5	0.658(4)	−7.7(4)	7.21(13)	2.29

[a] Parameter was fixed in the simulation.

Table S8. Zero-field splitting parameters determined on the basis of a modified spin Hamiltonian approach as described in the article main text. V_{IMP} denotes the volume fraction of a paramagnetic ($S = 1/2$) impurity.[a]

compound	$|D|$ (cm^{-1})	E/D (cm^{-1})[b]	g (1)	D_{TIP} (10^{-4} cm^3 mol^{-1})	V_{IMP}
4	55.0	0	1.487	9.63	5.3%
4'	56.1	0	1.687	7.16	5.1%
5	49.8	0	1.596	6.92	10.4%

[a] The determined g values of this analysis are unexpectedly small (g_{av} = 1.487–1.687) and cannot be physically explained. Most probably, this is a consequence of either weighing errors, partially sample decomposition or the presence of spin-orbit coupling. Therefore, although the simulation of the temperature-dependent effective magnetic moment resulted in an excellent agreement with the experimental data, we would like to stress that the obtained ZFS parameters of this analysis represent only an estimate with a relatively large uncertainty.

[b] The rhombic ZFS parameter E/D was fixed in the simulation (E/D = 0) because the free fit resulted in implausible values for E/D that strongly depend on the selection of the starting value.
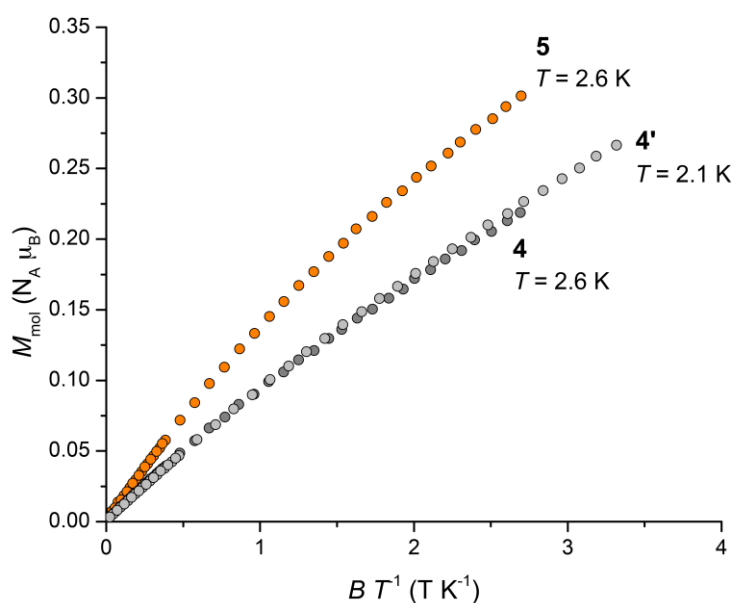
Figure S16. Magnetic field-dependent molar magnetisation (M_{mol}) for complexes **4** (dark grey), **4'** (grey) and **5** (orange) measured with an externally applied magnetic field between B_{ext} = 0.05 and 7 T at T = 2.1 or 2.6 K.

Decomposition studies

The magnetic measurements allowed the study of the decomposition of **4** and **5** by increasing the temperature above 300 K, giving a half-life of $t_{1/2} = 287$ min (**4**, $T = 310$ K) and $t_{1/2} = 138$ min (**5**, $T = 300$ K) (Figures S16–S17). Interestingly, a magnetic moment of about 2 μ_B, typically found for $S = 1/2$ systems, was still observed even after the sealed samples were kept several days at room temperature. This would imply a Mo(V) d^1 species, but all attempts to identify the decomposed substances have failed so far.
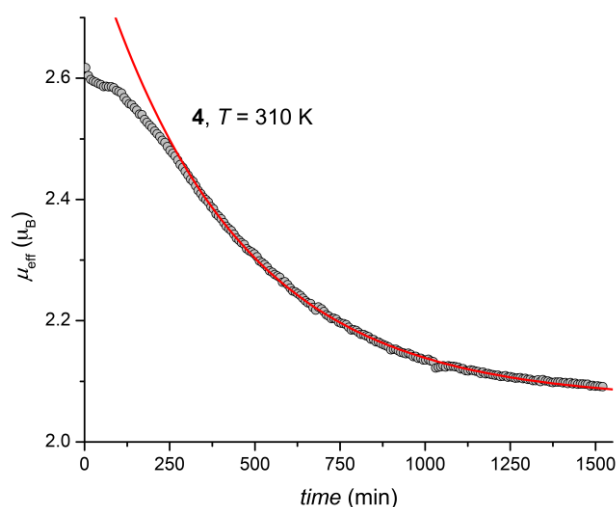
Figure S17. Effective magnetic moment (μ_{eff}) vs. *time* plots for complex **4** measured with an externally applied magnetic field of $B_{ext} = 0.1$ T at $T = 310$ K; symbols: experimental data; line: fit on the basis of an exponential decay model.
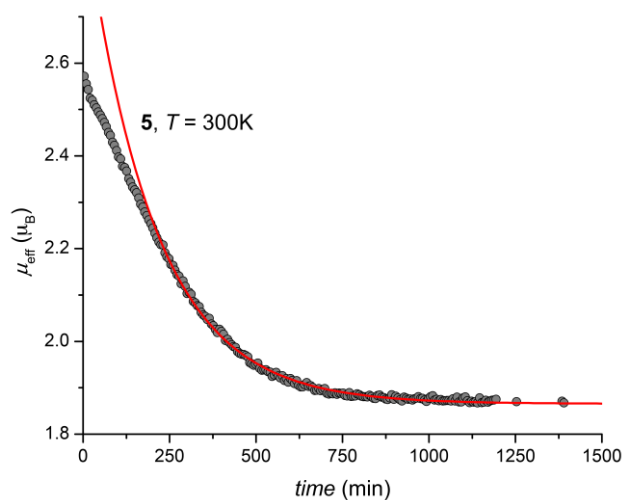
Figure S18. Effective magnetic moment (μ_{eff}) vs. *time* plots for complex **5** measured with an externally applied magnetic field of $B_{ext} = 0.1$ T at $T = 300$ K; symbols: experimental data; line: fit on the basis of an exponential decay model.

Computational studies

Table S9. Absolute electronic and thermodynamic data computed at the B3LYP/6-311G(d,p) level of theory. For some compounds both the singlet and the triplet state were calculated. All values are given in atomic units (Hartree).

Compound	E_0	E_{298}	H_{298}	G_{298}
1 ($S = 0$)	−2941.962110	−2941.915320	−2941.914376	−2942.048310
2 ($S = 0$)	−657.193316	−657.176493	−657.175549	−657.239643
3 ($S = 0$)	−502.381096	−502.364890	−502.363946	−502.427100
4 ($S = 0$)	−3599.190659	−3599.127148	−3599.126203	−3599.294018
4 ($S = 1$)	−3599.206587	−3599.142738	−3599.141794	−3599.312276
5 ($S = 0$)	−3444.366056	−3444.303738	−3444.302794	−3444.468414
5 ($S = 1$)	−3444.38725	−3444.324866	−3444.323922	−3444.489241
I1 ($S = 0$)	−3599.176261	−3599.112922	−3599.111978	−3599.278569
I1 ($S = 1$)	−3599.180596	−3599.117320	−3599.116375	−3599.284725
I2 ($S = 0$)	−716.200088	−716.180936	−716.179991	−716.249307
I3 ($S = 0$)	−2882.976335	−2882.931941	−2882.930997	−2883.061185
I4 ($S = 0$)	−3444.354782	−3444.293001	−3444.292056	−3444.453644
I4 ($S = 1$)	−3444.360986	−3444.298665	−3444.297721	−3444.462846
I5 ($S = 0$)	−638.793451	−638.774376	−638.773431	−638.844988
I6 ($S = 0$)	−2805.570664	−2805.526542	−2805.525598	−2805.655702
I7 ($S = 0$)	−3599.125298	−3599.061767	−3599.060823	−3599.225748
1N ($S = 0$)	-3658.158959	-3658.093091	-3658.092147	-3658.264554
1N ($S = 1$)	-3658.172199	-3658.105959	-3658.105014	-3658.279044
3N ($S = 0$)	-3540.195009	-3540.134223	-3540.133279	-3540.294687
3N ($S = 1$)	-3540.212153	-3540.151028	-3540.150084	-3540.313764

Table S10. Relative electronic and thermodynamic data computed at the B3LYP/6-311G(d,p) level of theory. All values are given in kcal mol^{-1}.

Compound	ΔE_0	ΔE_{298}	ΔH_{298}	ΔG_{298}
4 ($S = 0$)	9.99	9.78	9.78	11.46
4 ($S = 1$)	0.00	0.00	0.00	0.00
I1 ($S = 0$)	19.03	18.71	18.71	21.15
I1 ($S = 1$)	16.31	15.95	15.95	17.29
I7 ($S = 0$)	51.01	50.81	50.81	54.30

Table S11. Relative electronic and thermodynamic data computed at the B3LYP/6-311G(d,p) level of theory. All values are given in kcal mol^{-1}.

Compound or reaction	ΔE_0	ΔE_{298}	ΔH_{298}	ΔG_{298}
1 ($S = 0$) + **2** ($S = 0$) [+ **2** ($S = 0$)]	0.00	0.00	0.00	0.00
I1 ($S = 1$) [+ **2** ($S = 0$)]	−15.79	−16.01	−16.60	2.03
I2 ($S = 0$) + **I3** ($S = 0$) [+ **2** ($S = 0$)]	−13.18	−13.22	−13.22	−14.14
4 ($S = 1$) [+ **2** ($S = 0$)]	−32.10	−31.96	−32.55	−15.26
0.5 **3N** ($S = 1$) + 0.5 **1N** ($S = 1$) [+ **2** ($S = 0$)]	−23.06	−23.02	−23.61	−5.30
3N ($S = 1$) + **I2** ($S = 0$)	−39.85	−39.95	−40.45	−22.26
I7 ($S = 0$) [+ **2** ($S = 0$)]	18.91	18.85	18.26	39.03

Table S12. Relative electronic and thermodynamic data computed at the B3LYP/6-311G(d,p) level of theory. All values are given in kcal mol^{-1}.

Compound	ΔE_0	ΔE_{298}	ΔH_{298}	ΔG_{298}
5 ($S = 0$)	13.30	13.26	13.26	13.07
5 ($S = 1$)	0.00	0.00	0.00	0.00
I4 ($S = 0$)	20.37	20.00	20.00	22.34
I4 ($S = 1$)	16.48	16.44	16.44	16.56

Table S13. Relative electronic and thermodynamic data computed at the B3LYP/6-311G(d,p) level of theory. All values are given in kcal mol^{-1}.

Compound or reaction	ΔE_0	ΔE_{298}	ΔH_{298}	ΔG_{298}
1 ($S = 0$) + **3** ($S = 0$)	0.00	0.00	0.00	0.00
I4 ($S = 1$)	−11.16	−11.58	−12.17	7.88
I5 ($S = 0$) + **I6** ($S = 0$)	−13.12	−12.99	−12.99	−15.86
5 ($S = 1$)	−27.64	−28.02	−28.61	−8.68
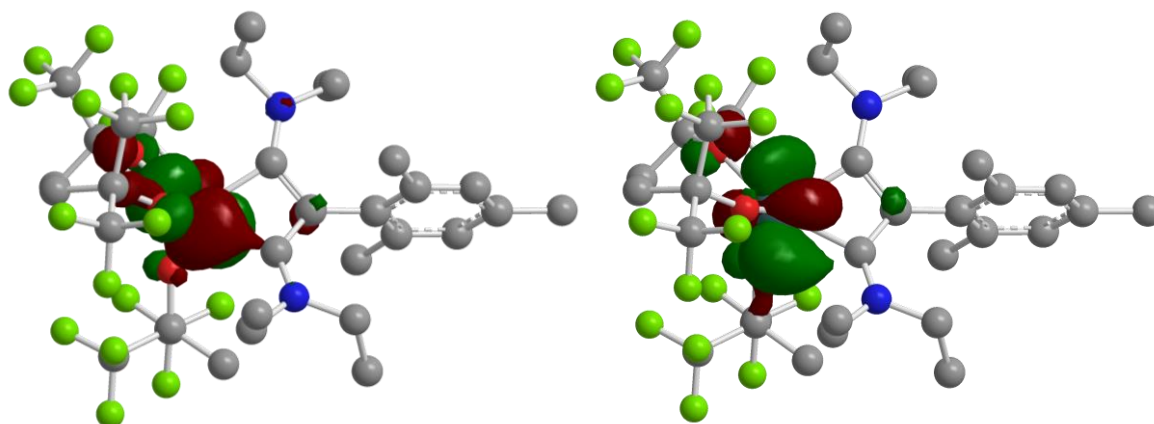
Figure S19. Contour plots (isovalue = 0.40) of the biorthogonalised SOMO (left) and SOMO−1 (right) of complex **5**.

LUMO+6

LUMO+5

LUMO+2

LUMO+1

LUMO

HOMO−2

HOMO−5

HOMO−7
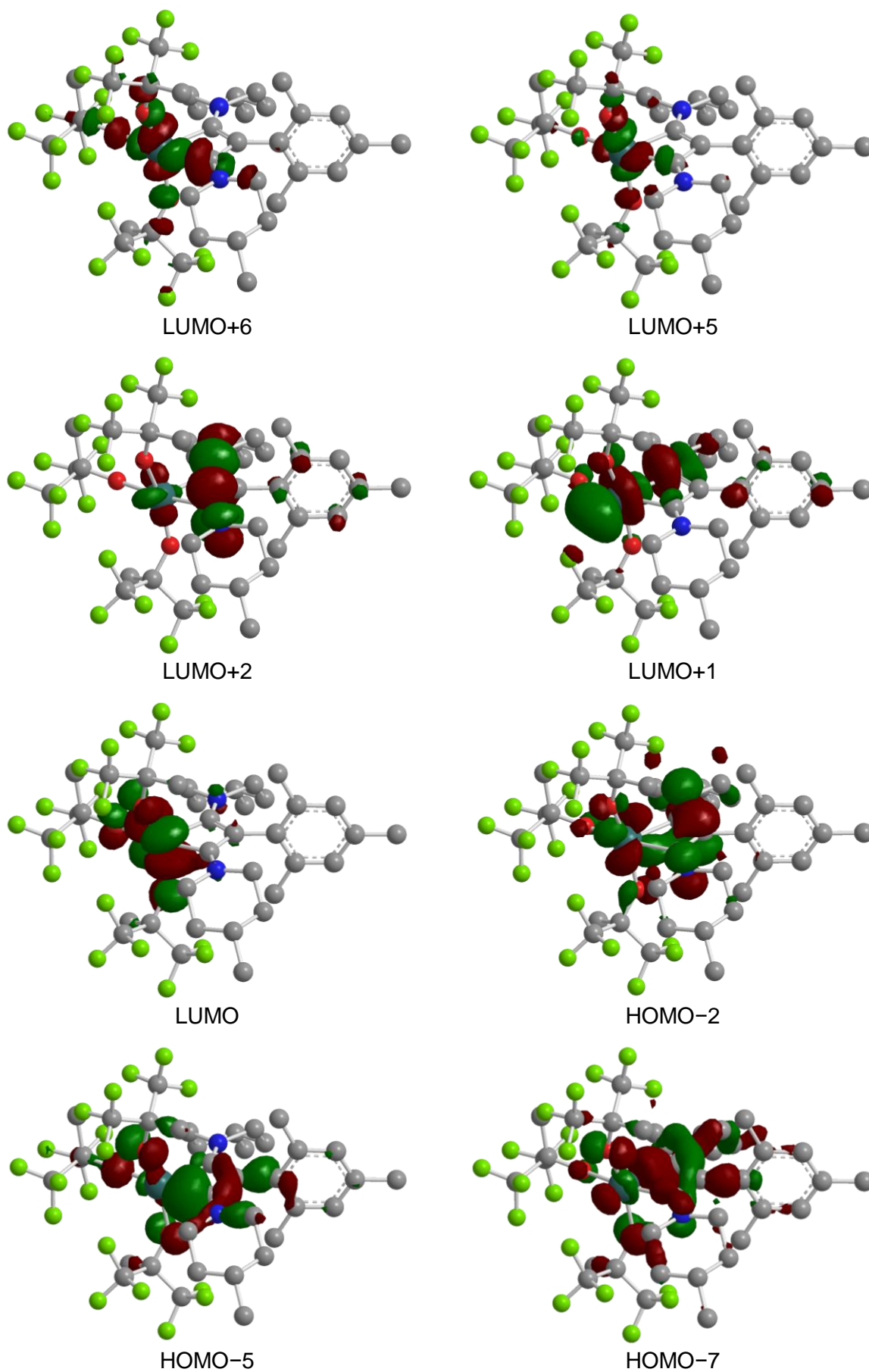
Figure S20. Contour plots (isovalue = 0.40) of selected molecular orbitals of complex **4**.
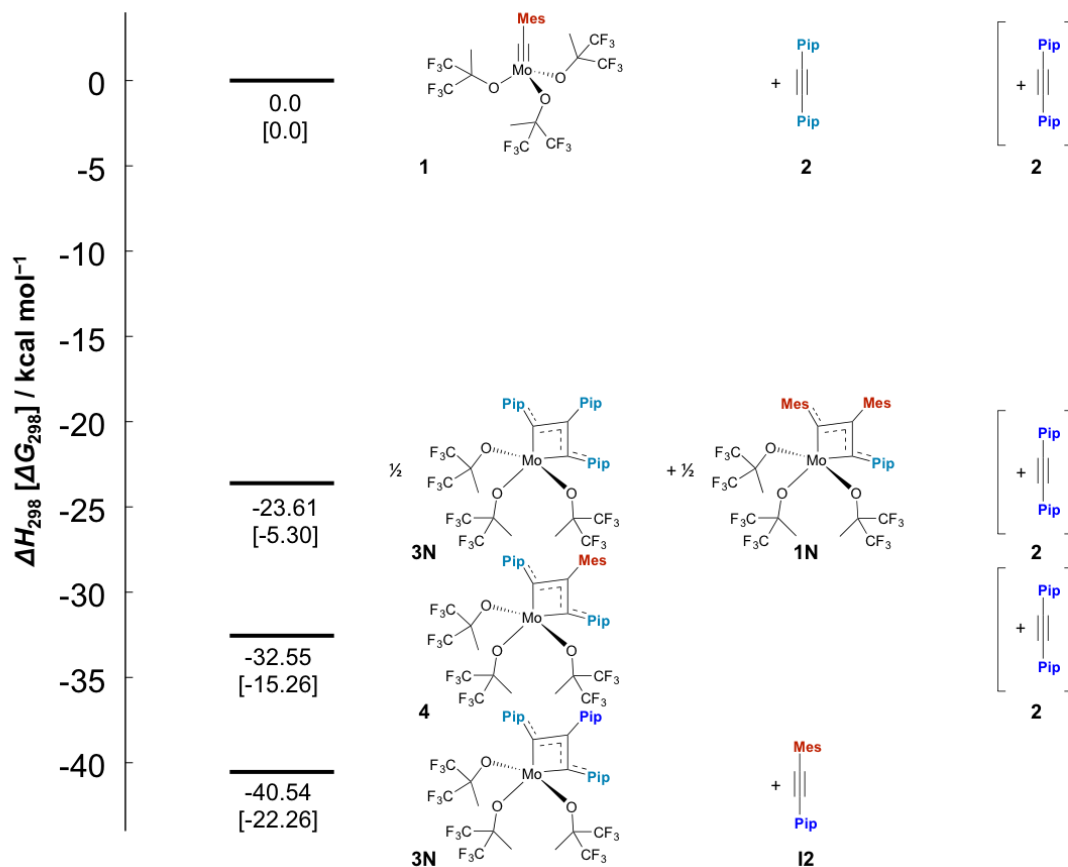
Figure S21. Relative reaction enthalpies/free energies of possible products of the reaction of **1** with either one or two equivalents of **2**. The formation of the triaminospecies **3N** is thermodynamically preferred only in the presence of two equivalents of **2**, whereas the diaminospecies is preferred in the presence of only one equivalent of **2**.

References

1. A. R. Petrov, C. G. Daniliuc, P. G. Jones and M. Tamm, *Chem. Eur. J.*, 2010, **16**, 11804–11808.
2. G. Himbert, H. Naßhan and S. Kosack, *Synlett*, 1991, 117–118.
3. S. R. Klopfenstein, C. Kluwe, K. Kirschbaum and J. A. Davies, *Can. J. Chem.*, 1996, **74**, 2331–2339.
4. C. J. Adams, K. M. Anderson, I. M. Bartlett, N. G. Connelly, Orpen, A. Guy, T. J. Paget, H. Phetmung and D. W. Smith, *J. Chem. Soc., Dalton Trans.*, 2001, 1284–1292.